ASSIGNMENT REPORT

ON

"ELECTRODE BASED BLOOD GAS SENSORS"

BY:

GROUP 10

Nitin Pant (2018A8PS0381P)

Ayush Agrawal (2018A8PS0469)

Pranamya Jain (2018A8PS0769P)

NOVEMBER, 2020

TABLE OF CONTENTS

1. Introduction

The concentration of certain gases like O_2, CO_2 in the bloodstream of a human-beings is considered a vital stat in medical science that needs to be measured constantly for emergency and intensive care patients. Instrument required for the same must be very accurate and sophisticated to accurately analyze blood gas composition. The blood gas sensors that are being used now a days are the result of many years of gradual improvements and optimizations. The operating principles behind sensor technology have largely remained unchanged, but the size of analysers and sensors has decreased remarkably. Though in past few years new sensors based on micro-electromechanical systems, optical fibers etc. have come up thus making the analysis process faster and non-invasive at the same time.

The first blood gas sensor developed was a pH electrode. It was discovered that when there is a thin glass membrane separating two solutions of different pH, the system could generate a small potential difference. Though detection of this minute voltage was difficult at that time, as the advancements in electronics began, it became feasible to extract the voltage and process information using it.

Almost half a century later, American scientists, Stow and Severinghaus discovered a similar phenomenon to measure CO2 concentration (pCO2). Soon after, L.C. Clark constructed the Clark electrode, which could estimate the concentration of O2 in a solution. Finally, all three sensors were combined in one instrument by J.W. Severinghaus, making it the first blood gas analysis system in 1957 and 1958. Around the same time-period, Blood Oximetry began to come into existence. Millikan (in 1942) coined the term oximeter for a device he invented to measure Oxygen saturation in the ear of aviators losing consciousness at higher altitudes. This technique used optical analysis of the blood sample using a spectroscope to find Oxygen's saturation (SO2 or SaO2).

All the sensors mentioned above require blood to be extracted from the patient, i.e., these are invasive procedures and are sometimes associated with severe complications in the patient like infections, STD transmission, etc. Furthermore, as these procedures require sophisticated instruments and an environment to work with, the cost further increases. This has led to the advent for non-invasive techniques that can maintain the precision while being more cost-friendly and user-friendly. Also, the non-invasive method allows us to make real-time analysis possible and more comfortable.

In this report we mainly focus on electrode-based Blood Gas Sensors namely Severinghaus Electrode, Clark's Electrode. Subsequently we describe and study a semiconductor chip based on the above two electrode principles.

2. Severinghaus Electrode (CO2 Measurement)

2.1 Basics Principle & Working of Severinghaus Sensor:

The Severinghaus sensor is an electrode that is used to measure carbon dioxide (CO_2). It was developed by Dr. John W. Severinghaus and his technician A. Freeman Bradley. It consists of a CO_2-sensitive glass electrode in a surrounding film of bicarbonate solution covered by a thin plastic carbon dioxide permeable membrane, but impermeable to water and electrolytic solutes as it is known that CO2 cannot be reduced electrochemically in an aqueous solution. But CO2 levels can be determined indirectly by dissolving it in an aqueous electrolyte solution and then monitoring the resulting change in pH. The basic idea of the **membrane-covered potentiometric carbon dioxide sensor** consists of separating the sample being measured from the sensor's internal electrolyte solution by a thin rubber or polymer membrane, which is permeable to CO2 gas but not to ions or water.
The carbon dioxide pressure of a sample gas or liquid equilibrates through the membrane, and **the glass electrode measures the resulting pH of the bicarbonate solution**. Severinghaus carbon dioxide sensor, sometimes also called an electrode, is used to measure Co2 levels and is based on the above-stated principle. CO2 permeates from the gaseous or liquid specimen through the membrane into the spacer's electrolyte film until equilibrium between the CO2 partial pressure on both sides of the membrane has been established. During measurement, virtually no CO2 is consumed. In the sensor electrolyte, a series of equilibrium reactions occur, resulting in the formation of H+ ions and thus in a CO2-dependent shift of the pH value, which is measured using the integrated pH electrode.

2.2 Structure of Sensor:

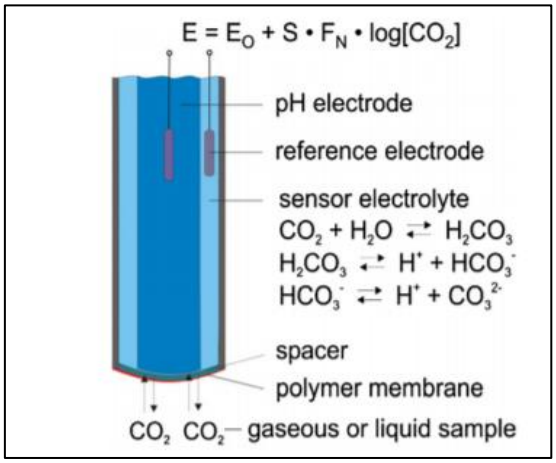

Figure 1. Severinghaus Electrode with Cathodic & Anodic Equations

The sensor's primary structure consists of a thin polymer membrane, the hydrogen carbonate containing electrolyte solution, a thin hydrophilic spacer sheet soaked with the electrolyte solution, and a pH probe.

Typical materials used as sensor membranes are polytetrafluoroethylene (PTFE), polymethyl pentene (TPX), silicone and polypropylene (P.P.). Their thicknesses range typically between 5 and 30 μm. To improve the mechanical stability, the thin membranes are often mechanically protected or reinforced by a perforated metal foil or other embedded compounds.

2.3 Mathematical Equations & Modelling of Sensor:

Since the concentration of H_2CO_3 (carbonic acid) in the sensor electrolyte is much lower than that of CO_2, the first two equations in figure 1 may be summarized as

$CO_2 + H_2O \equiv H^+ + HCO_3^-$ (bicarbonate ion) -(1)

The equilibrium is expressed by

$K_1 = \frac{[H^+][HCO_3^-]}{[CO_2]}$ -(2)

with K1 = 4.3 × 10−7 mol L−1 and pK1 = 6.36.

According to Henry's law, in the case of equilibrium between the gaseous and the liquid phases, the concentration of dissolved carbon dioxide [CO2] = c(CO2) in the sensor electrolyte is

$[CO_2] = K_H p(CO_2)$ -(3)

with KH = 3.4 × 10−2 (mol L−1) atm−1 (at 25 ◦C). p(CO2) is the partial pressure of CO2 in the sample (and finally also in the sensor electrolyte), and K.H. is the solubility coefficient of CO2:

$pH = -\log [H^+]$ -(4)

Inserting equations (3) and (4) in equation (2) and taking the logarithm results in the **Henderson–Hassel Balch equation** (25):

$pH = pK_2 + \log \frac{[HCO_3^-]}{K_H p(CO_2)}$ -(5)

Since the electrolyte of the Severing Haus carbon dioxide sensor already contains a large concentration of hydrogen carbonate, the changes in this concentration due to the dissociation of carbonic acid are negligible and thus the term $[HCO_3^-]$ can be regarded as a constant and added to pK2 in equation (5), resulting at last in the interesting dependence of the pH value on the partial pressure of CO2 in the sample:

$pH = K - \log\ p(CO_2)$ -(6)

The output voltage signal E of the pH electrode can be written as

$$E = E_1 - S \cdot F_N \cdot \mathrm{pH} = E_2 + S \cdot F_N \cdot \log\, p(\mathrm{CO_2}) \\ = E_0 + S \cdot F_N \cdot \log\,[\mathrm{CO_2}] \quad \text{-(7)}$$

Where $F_{.N.}$ is the Nernst factor (59.16 mV/decade at 25 ◦C), and S is the relative sensitivity of the carbon dioxide sensor, which practically ranges between 0.85 and 0.98.

In more details, the dependence of the CO2 sensor function on the NaHCO3 (sodium bicarbonate) concentration and the resulting Na+ concentration in the sensor electrolyte can be derived as follows:

$$\mathrm{HCO_3^-} \equiv \mathrm{H^+} + \mathrm{CO_3^{2-}}$$
$$K_2 = \frac{[\mathrm{H^+}][\mathrm{CO_3^{2-}}]}{[\mathrm{HCO_3^-}]} \quad \text{-(8)}$$

with K2 = 5.61 × 10−11 mol L−1 and pK2 = 10.25 (at 25 ◦C)

$$K_w = [\mathrm{H^+}] \cdot [\mathrm{O.H.^-}] \quad \text{-(9)}$$

with K_W = 1.008 × 10−14 (mol L−1) 2 (at 25 ◦C)

Introducing in the equation for charge neutrality

$$[\mathrm{H^+}] = [\mathrm{O.H.^-}] + [\mathrm{HCO_3^-}] + 2[\mathrm{CO_3^{2-}}] - [\mathrm{Na^+}] \quad \text{-(10)}$$

Results in:

$$[\mathrm{H^+}] = \frac{K_W}{[\mathrm{H^+}]} + \frac{K_1 K_H p(\mathrm{CO_2})}{[\mathrm{H^+}]} + \frac{2K_1 K_2 K_H p(\mathrm{CO_2})}{[\mathrm{H^+}]^2} - [\mathrm{Na^+}] \quad \text{-(11)}$$

$$[\mathrm{H^+}]^3 + [\mathrm{Na^+}][\mathrm{H^+}]^2 - \big(Kw + K_1 K_H p(\mathrm{CO_2})\big)[\mathrm{H^+}] \\ -2K_1 K_2 K_H p(\mathrm{CO_2}) = 0 \quad \text{-(12)}$$

For solving this equation Cardano's formula for a root of a cubic equation can be used with the following transformations:

$$[\mathrm{H^+}] = z - \frac{[\mathrm{Na^+}]}{3}$$

$$z^3 + pz + q = 0$$

$$p = -\big(K_w + K_1 K_H p(\mathrm{CO_2})\big) - \frac{[\mathrm{Na^+}]^2}{3}$$

$$q = \frac{2[\mathrm{Na^+}]^3}{27} + \frac{[\mathrm{Na^+}]\big(Kw + K_1 K_H p(\mathrm{CO_2})\big)}{3} \\ -2K_1 K_2 K_H p(\mathrm{CO_2})$$

The desired dependence of $[H^+]$ on the concentration of $[Na^+]$ is

$$[H^+] = \sqrt{-\frac{4}{3}}p \cdot \cos\left(\frac{1}{3}\arccos\left(-\frac{q}{2}\sqrt{-\frac{27}{p^3}}\right)\right) - \frac{[Na^+]}{3} \quad \text{-(13)}$$

The pH expression is given by,

$$pH = -\log[H^+] \quad \text{-(14)}$$

2.4 Sensitivity:

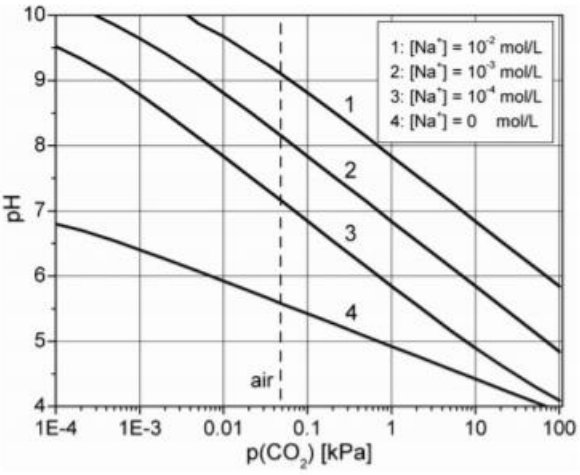

The sensitivity can be calculated as the slope of the graphs. Different graphs show variation with varying concentrations of NaHCo3 concentration in the sensor.

As previously stated, the Severinghaus electrode depends on the change in pH of the sample, resulting in potential between the electrodes. This change is then using equations is correlated to the CO_2 content of the blood. The pH calculated is then converted into voltage using the Nernst equation. In more detail the dependence of the CO_2 sensor function on the $NaHCO_3$ (sodium bicarbonate) concentration.

The sensor used when exposed to ambient air results in drying out of electrolyte filling, this raises a problem of multiple and frequent recalibrations. To prevent this, pH_2O (vapours) is decreased to a certain extent by adding ethylene glycol. This combined mixture does not influence the main sensor parameters significantly.

Apart from the mechanical, thermal, and electrical properties, the permeability for CO2 and H2O is essential for membrane material parameters. The permeabilities do not influence equilibrium-type sensors' sensitivity, but long-term behaviour and response time depend on them.

The temperature dependence of the permeability P can be calculated from the activation energy Ea using the following equation:

$$P = P_0 \cdot \exp\left(-\frac{E_a}{RT}\right).$$

The ratio of the membrane permeabilities for H2O and CO2 is of special importance regarding equilibrium-type carbon dioxide sensors' long-term stability. This parameter depends on the membrane material and amounts for silicone to p(H2O)/p(CO2) ≈ 13 and for polymethyl pentene to p(H2O)/p(CO2) < 1, which is therefore especially suited as membrane material for electrochemical CO2 gas sensors.

2.5 Dynamic Response of the Sensor:

The sensor's response depends on various factors like Thickness and the material of GPM (effecting the transport of CO_2 to the electrode), Thickness of the electrolyte film, concentrations of bicarbonates, and carbonic acids, etc.

Ross et al. has calculated the response time of this electrode with few assumptions. The equation of the response time is given as follows

$$t = \frac{lm}{Dk}\left[l + \frac{dc_B}{dc}\right] \ln \frac{\Delta c}{\varepsilon c_2}$$

With

$$\varepsilon = \left|\frac{c_2 - c}{c_2}\right|$$

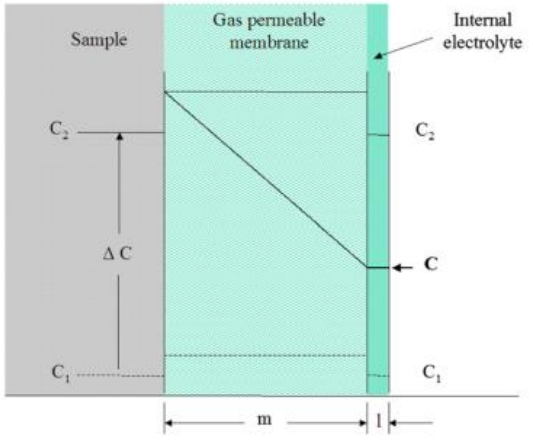

Figure Steady state model of the electrode response of the CO_2 electrode according to Ross

c_2 is the final concentration of H_2CO_3, c is the difference between the starting and end concentration of H_2CO_3, m is the Thickness of the membrane, and l is that of the inner electrolyte between electrode surface and membrane. D expresses the diffusion coefficient of the gas in the membrane, and k is the partition coefficient between the solution and the bulk of the membrane. The concentration-dependent dissociation of H_2CO_3 into HCO_3^- and CO_2^{3-} is described by the expression $\frac{dc_B}{dc}$. In c_B the ionic species are summarized. The factor ε gives the fractional approach of H2CO3 to the final concentration in the inner electrolyte. At higher concentrations of H_2CO_3, the relation $\frac{dc_B}{dc}$ is approximately constant in the equation, and the dependence of the time response can be estimated for different ratios of $c1/c2$.

2.6 Calibration:

Severinghaus-type sensors need to be calibrated very often to make the readings more accurate. As CO_2 based pH buffers solutions are not very stable, the buffer solution should be made just before starting the calibration process. To avoid larger temperature-dependent errors, the calibration solution's temperature should deviate by no more than 5 K from that of the measuring solution.

3. Clark Electrode (O2 Measurement)

3.1 Basics Principle & Working of Clark's Electrode:

Two electrode system, namely Ag and Pt electrodes
The external electrical circuit consists of a variable voltage source and an ammeter
The gas permeable membrane separating electrolyte from Oxygen sample (i.e. blood)
A cathode is made negative w.r.t anode until the dissolved O_2 molecules at cathode start getting reduced, resulting in an inflow of current in the external circuit
The magnitude of the current is proportional to the partial pressure of O_2.
The material used for membrane are polypropylene, polyethylene, Teflon, or Mylar
The rate of response of the electrode depends on the membrane thickness.

3.2 Structure of Sensor:

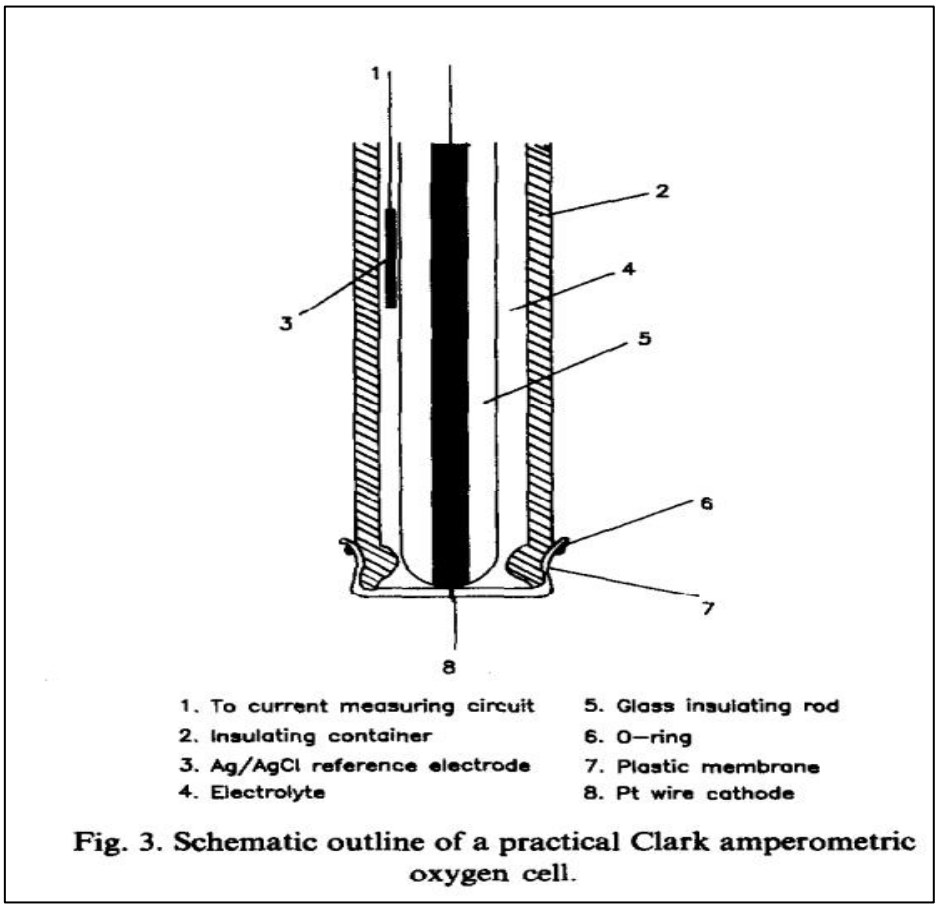

Fig. 3. Schematic outline of a practical Clark amperometric oxygen cell.

https://www.sciencedirect.com/science/article/abs/pii/0039914093800029
Amperometric gas sensors by S.C. Chang

3.3 Theoretical Considerations:

- Oxygen reduction is made using inert electrodes of Pt/Au and the reference electrode of Ag/AgCl or Calomel electrode in neutral KCl solution.
- The reaction at cathode and anode are as follows
- Cathode Reaction

$$O_2 + 2H_2O + 2e^- \rightarrow H_2O_2 + 2OH$$
$$H_2O_2 + 2e^- \rightarrow 2OH$$
Anode reaction: $Ag + Cl^- \rightarrow AgCl + e^-$
Overall reaction: $4Ag + O_2 + 2H_2O + 4Cl^- \rightarrow 4AgCl + 4O.H.^-$

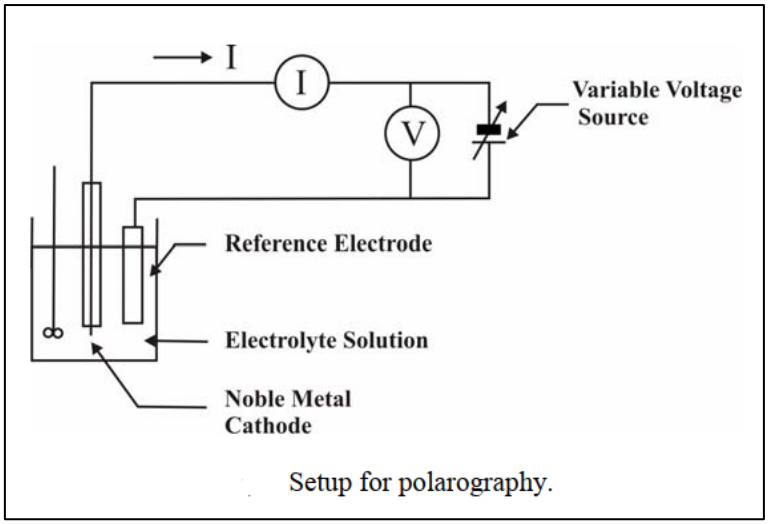

Setup for polarography.

3.4 Mathematical Equations & Modelling of Sensor:

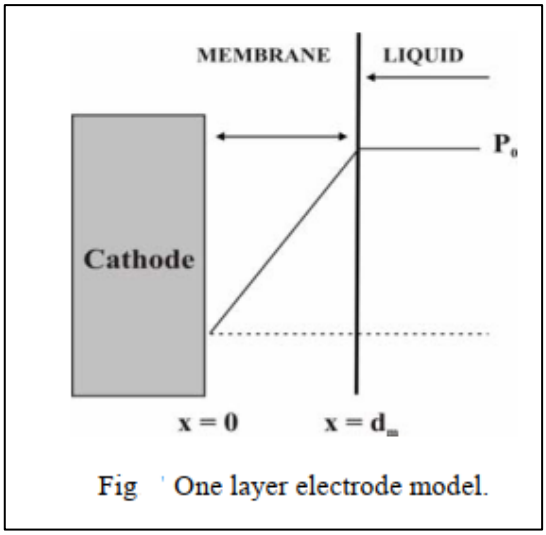

Fig One layer electrode model.

The above figures show two different models for the same sensor. The first one, i.e., the one-layer electrode model works with all three assumptions; however, the second assumption does not align with the practical situation. That is why a Two-layer model is used where the partial pressure of O_2 in the membrane is to be different from that of the liquid substrate.

Experimental data shows a 1-5% increase in sensor output current per $°C$ increase in temperature. D.O. sensor is Diffusion Oxygen Sensor.

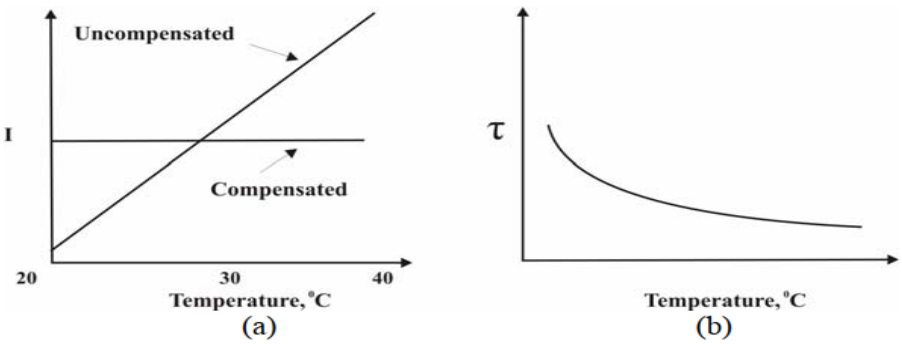

Fig Temperature dependency of DO sensor.

The sensor can be approximated as a first-order system:

$$c - c_p = \tau_p \left(\frac{dc_p}{dt} \right)$$

c- the oxygen concentration in the measurement sample; c_p - the oxygen concentration measured by the sensor; τ_p - the sensor time constant

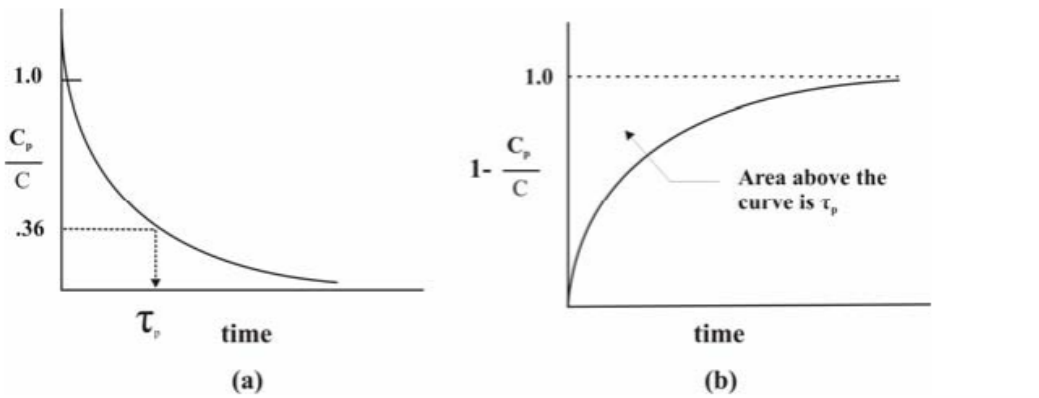

Fig. (a) Sensor response time measurement; (b) integral method for measuring the sensor time constant.

When the cathode diameter goes below 1μm the sensor renders insensitive to the liquid flow. Also as the area decreases the current also decreases, making the sensor susceptible to noise and decreasing its Signal to Noise ratio (SNR). Also, a trade-off is done between membrane thickness and the sensor's speed to make it more reliable.

3.5 Mathematical Modelling:

Fick's 2nd law describes the unsteady-state diffusion in the membrane:

$$\frac{\partial \mathrm{p}}{\partial t} = \mathrm{D_m}\frac{\partial^2 \mathrm{p}}{\partial \mathrm{x}^2} \quad (1)$$

D_m -the oxygen diffusivity in the membrane: x= the distance from the cathode surface. The initial and boundary conditions are

$$\mathrm{p} = 0 \text{ at } \mathrm{t} = 0 \quad (2)$$
$$\mathrm{p} = 0 \text{ at } \mathrm{x} = 0 \quad (3)$$
$$\mathrm{p} = \mathrm{p_0} \text{ at } \mathrm{x} = \mathrm{d_m} \quad (4)$$

d_m – the membrane thickness; p_0 – the partial pressure of Oxygen in the bulk liquid. The solution of the equation1 with the boundary condition is :

$$\frac{\mathrm{p}}{\mathrm{p_0}} = \frac{\mathrm{x}}{\mathrm{d_m}} + \sum_{\mathrm{n}=1}^{\infty} \frac{2}{\mathrm{n}\pi}(-1)^{\mathrm{n}} \sin\frac{n\pi x}{d_m} exp\left(-\frac{n^2\pi^2 D_m t}{d_m^2}\right) (5)$$

The current output of the electrode is proportional to the oxygen flux at the cathode surface:

$$\mathrm{I} = \mathrm{NFAD_m}(\partial \mathrm{C}/\mathrm{Ox})_{\mathrm{x}=0} = \mathrm{NFAP_m}(\partial \mathrm{p}/\partial \mathrm{x})_{\mathrm{x}=0} \quad (6)$$

N – number of electrons per mole of Oxygen reduced; F – faraday constant (= 96500 C/mol); A – surface area of the cathode; P_m – oxygen permeability of the membrane. The permeability of the membrane P_m is related to diffusivity by:

$$\mathrm{P_m} = \mathrm{D_m S_m} \ (7)$$

S_m – the oxygen solubility of the membrane

From EQs. (5) and (6), the current output It of the electrode is:

$$\mathrm{I_t} = \mathrm{NFA}\frac{\mathrm{P_m}}{\mathrm{d_m}}\mathrm{p_0}\left[1 + 2\sum_{\mathrm{n}=1}^{\infty} (-1)^{\mathrm{n}} \exp\left(-\mathrm{n}^2\pi^2\mathrm{D_m t}/\mathrm{d_m^2}\right)\right] \ (8)$$

The pressure profile within the membrane and the current output under steady-state conditions can be obtained from eqs. (5) and (8), respectively:

$$\frac{p}{p_0} = \frac{d}{d_m} \ (9)$$

And $$I_s = NFA\frac{p_m}{d_m}p_0 (10)$$

3.6 Calibration of Clark Electrode:

- In the beginning of the reduction process, current increases and as the time goes by it starts settling to a constant value
- On further increasing the bias, the electrode's current output rises rapidly due to other reactions, primarily the reduction of water to hydrogen.
- Relative current output vs % Oxygen yields linear characteristic curve for the voltage applied in the plateau region of the current close production vs Negative bias voltage

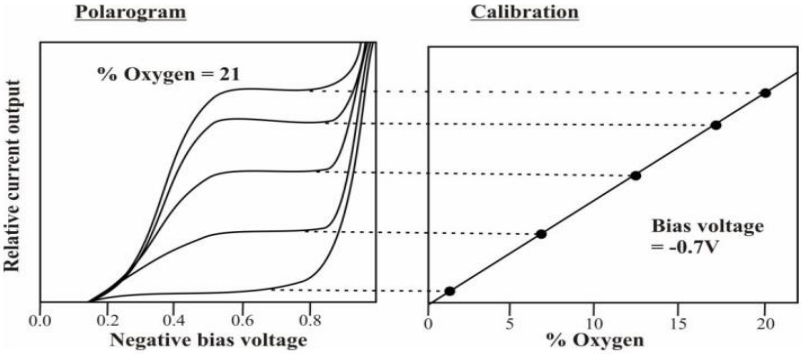

Using these plots, the sensor is calibrated before using

- To get the sensor output characteristics of Clark electrode (One-Layer Model) few assumptions are made
    - i. Cathode is well-polished, and the membrane is not loose. Also, it is assumed that the Thickness of electrolyte layer between membrane and cathode is negligible.
    - ii. Partial pressure of O_2 is same at the membrane surface as well as bulk liquid
    - iii. O_2 diffusion occurs only perpendicular to the membrane.

4. Combined Blood Gas Sensor:

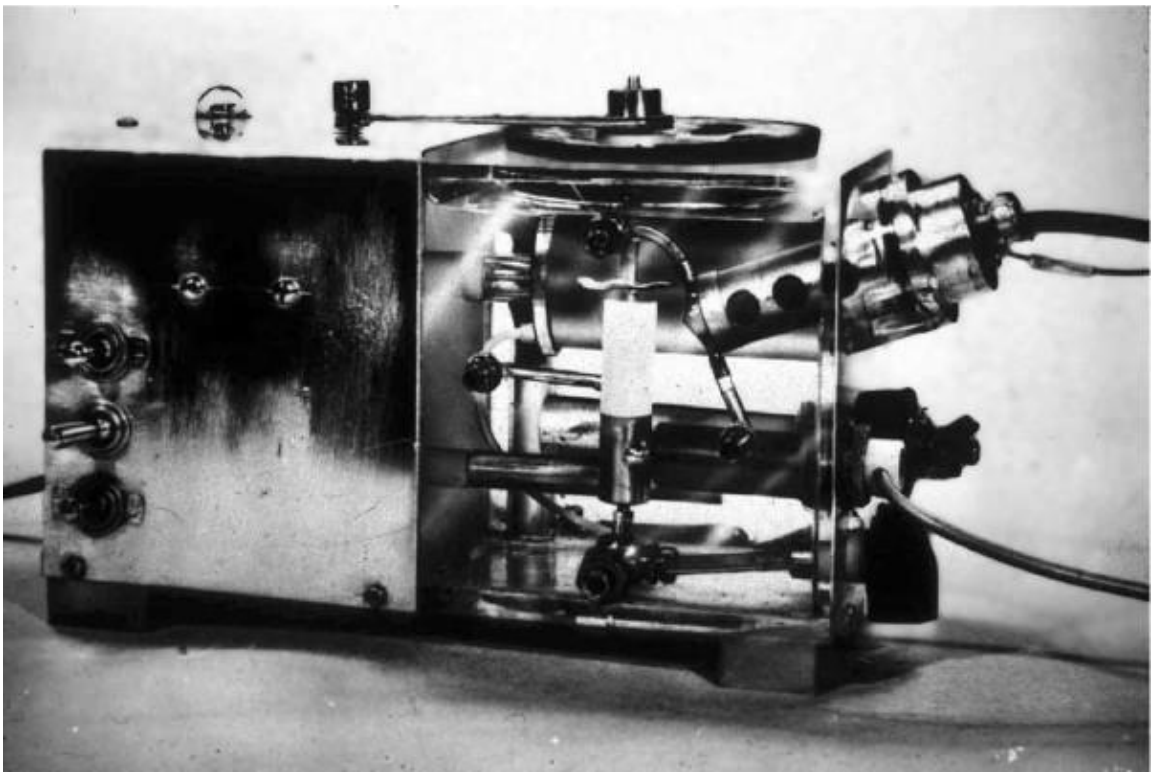

Above pictures shows the first combined blood gas sensor assembled together by Severinghaus in late 1950s.

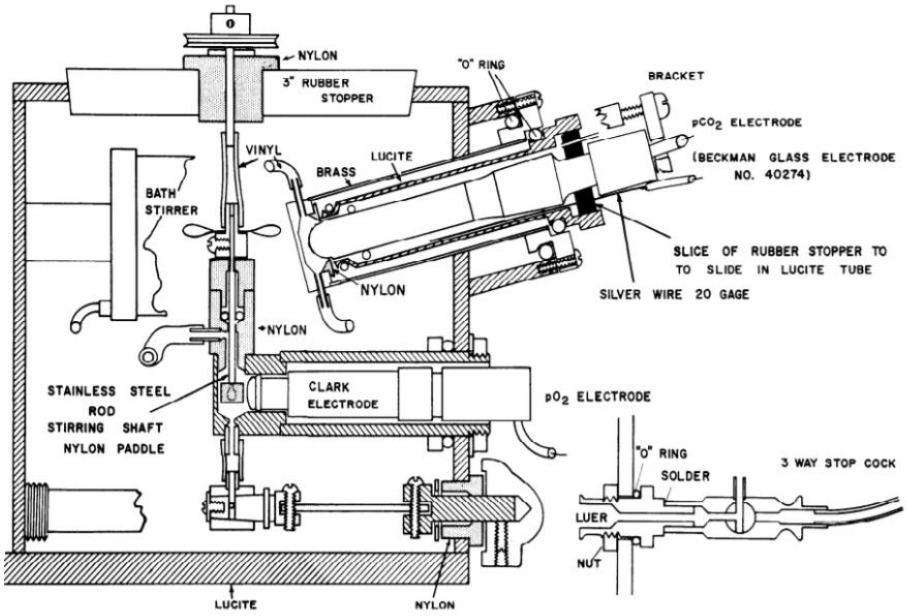

FIG. Construction of cuvettes and CO_2 electrode.

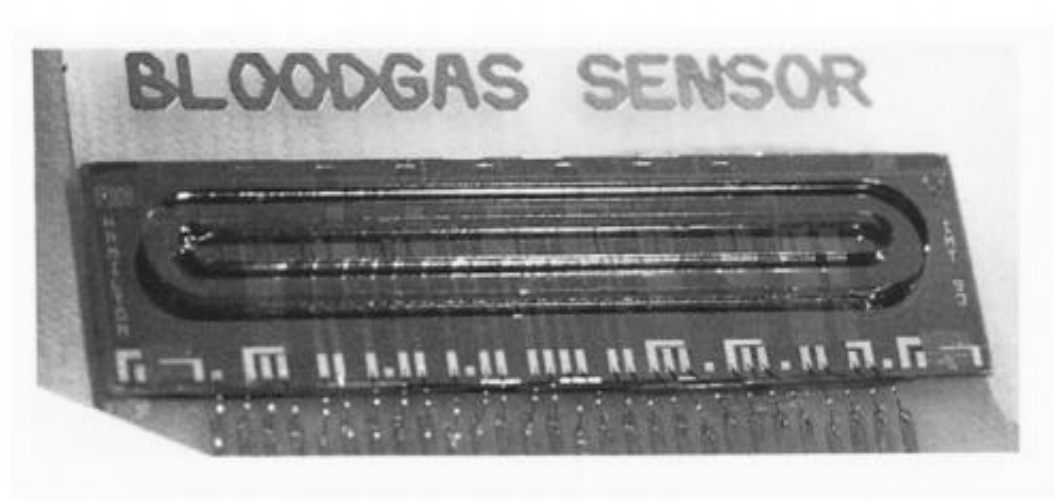

In early 1995 Ph. Arquint and his colleagues, B.H. van der Schoot and N.F. de Rooij, took the severinghaus machine's basics and miniaturized it at an I.C. chip level using ISFETs.

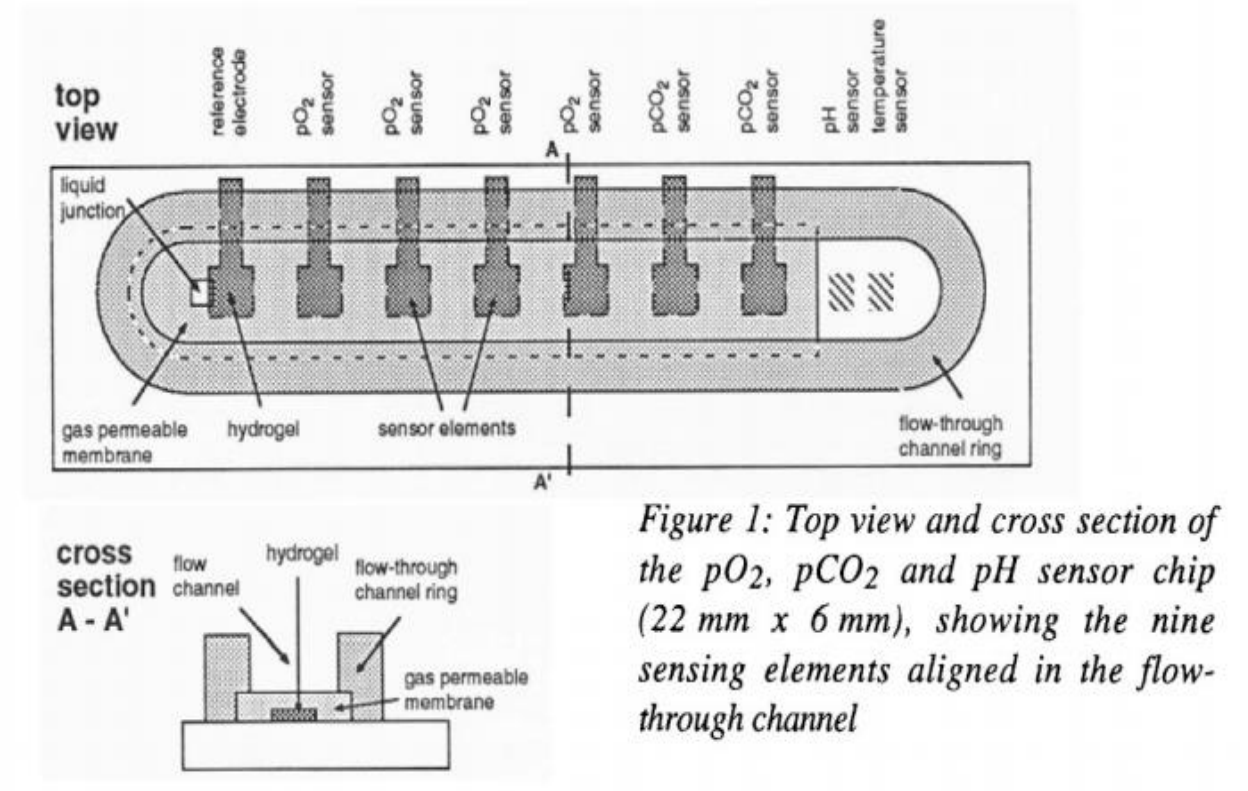

Figure 1: Top view and cross section of the pO_2, pCO_2 and pH sensor chip (22 mm x 6 mm), showing the nine sensing elements aligned in the flow-through channel

Image source: COMBINED BLOOD GAS SENSOR FOR p02, pC02, AND pH
Ph. Arquint, B.H. van der Schoot and N.F. de Rooij

4.1 Sensor Chip Design and Fabrication:

A Miniaturized silicon-based sensor chip. Sensor fabrication is based on wafer-level using IC-based technologies. The electrochemical cell is made using Ion-Sensitive Field Effect Transistors (ISFETs). The sensing channel has an Internal volume of $15\mu l$. A total of 9 sensing elements comprise four amperometric pO2 sensors, 2 ISFET-based pCO_2, pH-ISFET sensor, and one temperature sensor. The Clark-type pO_2 sensor has 9×8 small Pt-electrodes with $5\mu m$ in diameter spaced at $100\mu m$. They all are connected in parallel. Both Pt and Ag/AgCl electrodes are covered with lead and are separated from the sample using the Gas Permeable Membrane. The Severinghaus pCO_2 sensor is made using pH-ISFET and Ag/AgCl reference electrode, covered with Hg and GPM. The pH sensor has a similar structure to that of pCO_2 but has a fissure in the permeable membrane of $0.5\mu m \times 0.5\mu m$ dimension, which is used as the liquid junction.

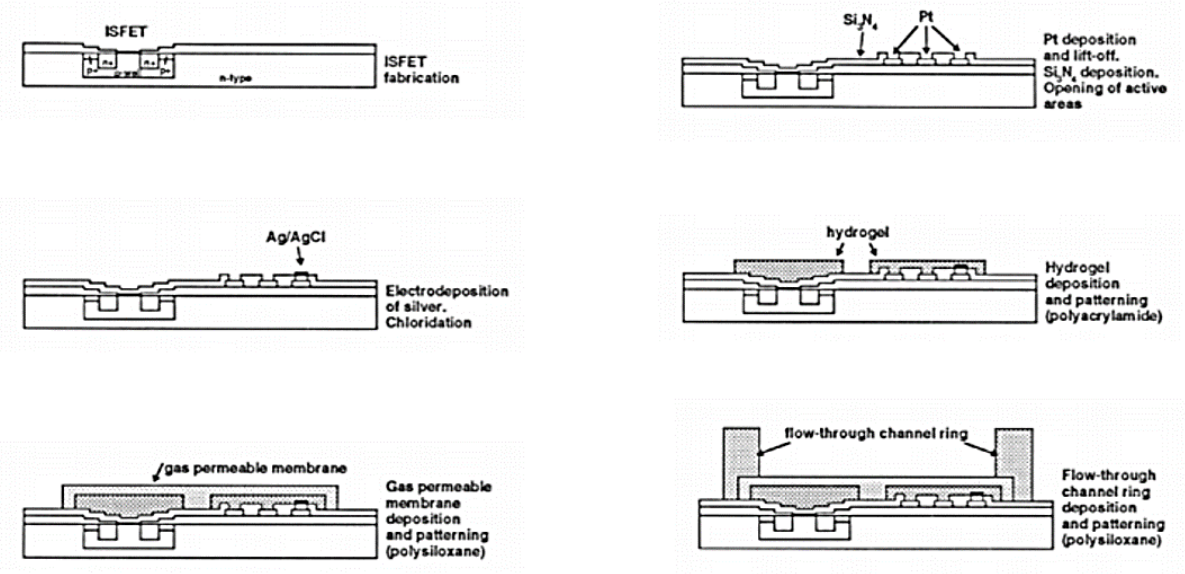

Oxygen Sensor:

This is a miniaturized amperometric Clark-type sensor which has three thin-film electrodes. The working (WE) and counter electrode (C.E.) material are Pt (Platinum), whereas the reference electrode (RE) is an Ag layer covered with AgCl. The electrodes are set in a concentric arrangement with RE in the centre($0.125mm^2$), the C.E. around it ($1\ mm^2$), and the WE as the outer ring($0.5mm^2$)

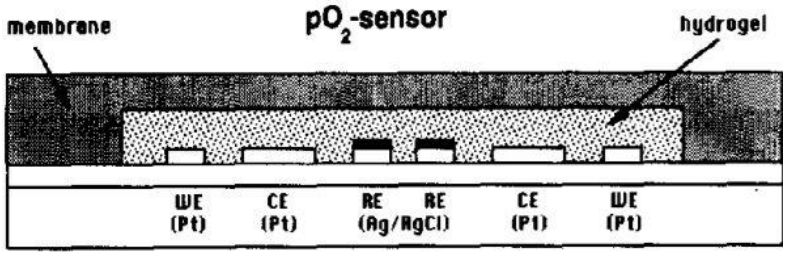

A polyacrylamide hydrogel layer containing 100 mM KC1 is made to cover the electrodes and thus helps in serving as an internal electrolyte. The hydrogel is separated from the sample by an outer gas-permeable polysiloxane membrane (Fig. 2). In operation, the WE are held at -700 mV versus the RE to perform the 0_2 reduction at the WE:

$$O_2 + 2H_2O + 4e^- \rightarrow 4H^+$$

Carbon di-oxide sensor:

The pCO_2 sensor is of the Severinghaus type and uses an Al_2O_3-ISFET and a thin-film Ag/AgCl reference electrode (RE). Both the ISFET and the RE are covered by a polyacrylamide hydrogel layer containing a 50 mM bicarbonate solution. The hydrogel is separated from the sample by a polysiloxane membrane. CO_2 diffuses through the membrane into the hydrogel, and the resulting pH variation of the bicarbonate solution is detected by the ISFET. Due to the hydration of CO_2 and the dissociation equilibrium of carbonic acid, there is a resulting pH change

$$CO_2 + H_2O \leftrightarrow H_2CO_3 \leftrightarrow H^+ + HCO_3^-$$

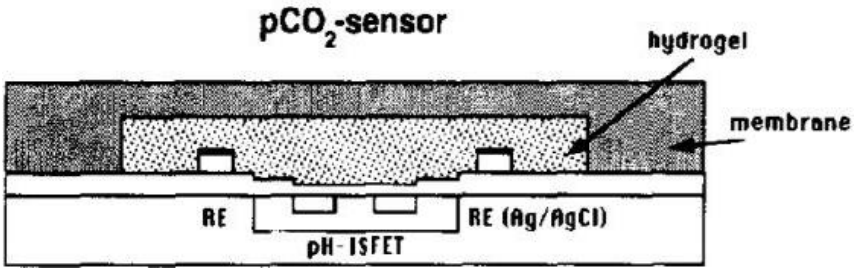

pH sensor:

The pH of the sample is measured by an Al_2O_3- ISFET with a thin film Ag/AgCl reference electrode (RE). The gate of the ISFET is in direct contact with the sample, while the RE is covered by a hydrogel layer containing a 100 mM KCl solution. The hydrogel is separated from the sample by an outer polysiloxane membrane. A small opening in this membrane serves as a liquid junction

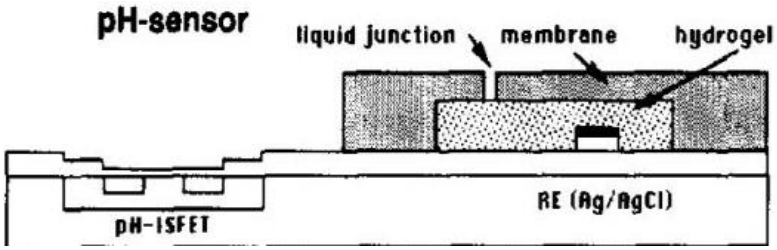

4.2 Characterization of the sensor:

A detailed characterization concerning the sensitivity, response time, stability, lifetime, temperature dependence, and the three sensors' mutual interference has been performed in an aqueous solution. In

the second step, the sensor has been tested in vitro using blood intended initially for transfusion, obtained from the Hospital des Cadolles in Neuchatel. The plasma is replaced by an anticoagulant solution (citrate phosphate dextrose CPD), which is a standard method for collecting blood for transfusion. This procedure reduces the calcium ion concentration, thus inhibiting blood clotting and haemolysis. For the aqueous solution measurements, the samples are equilibrated with $O_2/CO_2/N_2$ gas mixtures and then measured in a flow-through cell. The blood samples (8 ml) are equilibrated for 30 min with humidified O_2/ CO_2/N_2 gas mixtures using an IL 237 tonometer from Instrumentation Laboratories. Between the blood measurements, the flow-through system is rinsed with a 100 mM KCl solution equilibrated with N_2

Results:

Figure 4 shows the calibration curve of the $p0_2$ sensor in a solution containing 50 mM $NaHCO_3$, 50 mM NazC03, and one mM KCl saturated with O_2/N_2 gas mixtures.

The sensor exhibits a sensitivity of 5 nA/ mmHg for O-150 mmHg 0_2 partial pressures and a 95% response time (T_{95}) of 1 min with a sample flow velocity of 5 ml/min.

The sensor can be operated continuously for more than two weeks, with the stability of +-2%. The temperature coefficient is 1%/°C.

When the flow rate is doubled, the current increases by 2-3%. The CO_2 effect on the 0_2 response is 4-5% when the CO_2 partial pressure is doubled.

Figure 5 is the calibration curve of the $p0_2$ sensor in blood for transfusion at 37 "C and at a sample flow of 0.4 ml/min. The sensitivity is 6 nA/mmHg for O-200 mmHg 0_2 partial pressures and T_{95} is about 10 min.

The slight non-linearity and the slow T_{95} are probably due to the gas permeability of the tubings and of the flow-through cell itself, which decreases the 0_2 partial pressure at the sensor surface, especially at a low sample velocity.

It should be noted that between the blood samples, the flow-through system is rinsed using a solution equilibrated with N_2

Figure 6 shows the calibration curve of the $pC0_2$ sensor in a 100 mM KCl solution saturated with CO_2/ N_2 gas mixtures. These measurements are performed in an unstirred solution. The sensitivity is -49 mV/decade for CO_2 partial pressures between 0 and 150 mmHg and T_{95} is 2 min. The sensor is stable for more than 2 weeks under continuous operation with a drift of about 1-2 mV/day. The temperature coefficient is 0.7 mV/°C The output of the sensor is not affected by pO_2 and pH changes of the sample.

is the calibration curve of the $pC0_2$ sensor in blood for transfusion at 37 °C and at a sample flow of 0.4 ml/mm The sensitivity is - 52 mV/dec for 4-150 mmHg CO2 partial pressures and T_{95} is about 5 min. The slight non-linearity above 100 mmHg and below 5 mmHg and the slow T_{95} have the same origin as mentioned in the case of the $p0_2$ sensor.

For the pH sensor in aqueous solution a sensitivity of 53 mV/pH is found in the clinically important range (Fig. 8). The sensitivity is linear for pH 1-13. The drift is 1-2 mV/day and T_{95} a few seconds. The temperature coefficient is +0.8 mV/°C. There is no interference of either pO_2 or $pC0_2$ on the pH response.

It should be noted that in KCl-free solution, the drift of the reference electrode due to the KCl loss through the liquid junction is about 0.1 mV/min.

Intermittent flow-through measurements using two phosphate buffers at pH 7.0 and 7.4 with a KC1 concentration of 100 mM and blood for transfusion give very reproducible results with a standard deviation of 0.2 mV.

The characterization of the three sensors concerning sensitivity, response time and drift in aqueous solutions and in transfusion blood has shown promising results. The next step of the project will consist of clinical tests with whole blood.

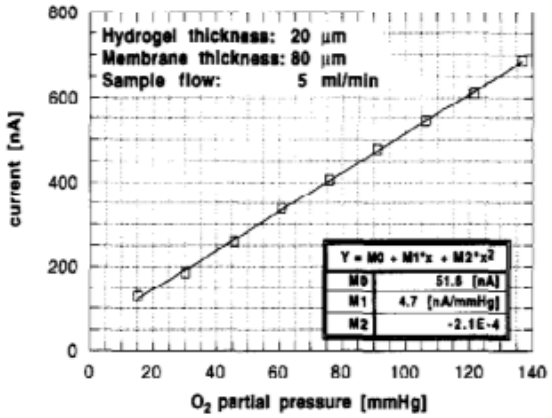

Fig. 4. p02 sensitivity in a solution containing 5O mM $NaHCO_3$, 50 mM Na_2CO_3 and 1 mM KCL saturated with different $0_2/N_2$ gas mixtures, sample flow: 5 ml/min, room temperature.

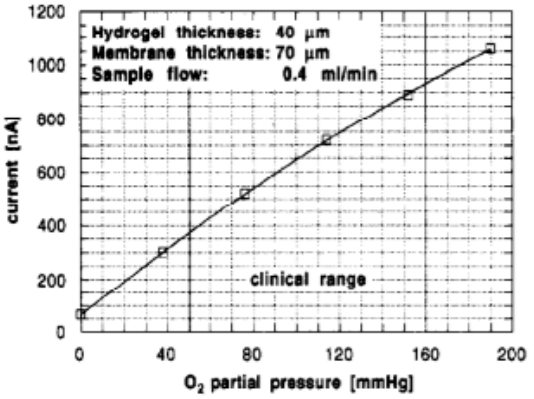

Fig. 5. pO_2 sensitivity in blood for transfusion at 37 °C saturated with different $0_2/N_2$ gas mixtures, sample flow: 0.4 ml/min.

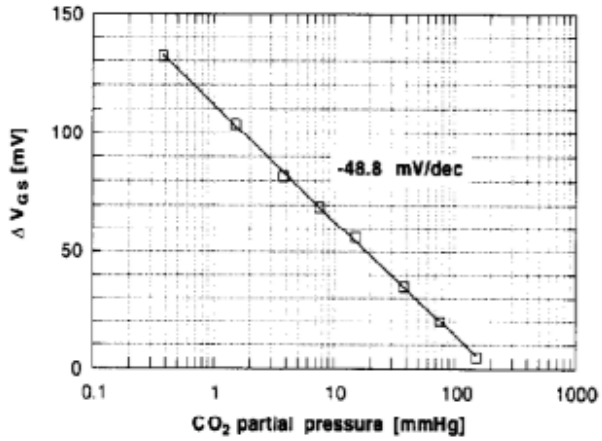

Fig. 6. pCO_2 sensitivity in a 100 mM KCL solution saturated with different C02/N2 gas mixtures; room temperature.

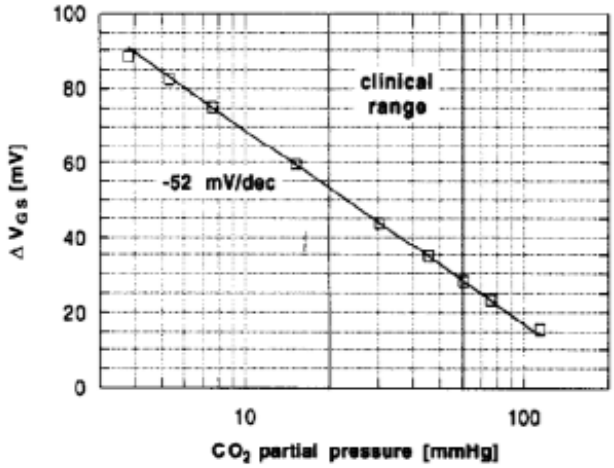

Fig. 7. pCO_2 sensitivity in blood for transfusion at 37 C saturated with different C02/N, gas mixtures, sample flow: 0.4 ml/min.

5. Learning Outcomes:

pH and blood gas sensing are indispensable tool in every intensive care unit. For patients with acute phase of respiratory failure or who are supported by mechanical ventilation, multiple blood gas analyses at short intervals are required. Thus, this intrigued our interest as in how various sensors have been able to help us ease out these processes. This assignment turned out be a great learning opportunity for our team. We got to review various sensors used for blood gas sensing, we could understand them better due to previous exposure to TMT concepts. We got to learn about the basic working principle and structures of various blood gas sensors that have developed and have been evolving over time. These included:

1) Severing Haus Sensor
2) Clark Sensor
3) Combined Blood Sensor

We also go to learn about the mathematical modelling and theoretical assumptions that go into building such intricate sensors. We got to know about the procedure of calibration of these sensors and were able to appreciate their modelling. We also got to learn about various conditions and limitations one has to take care while calibrating and using these sensors. At this point of time we are familiar with the pros and cons of such invasive and continuous methods, thus have an idea of what future research in this field might be related to.

Pros of continuous and invasive methods of blood gases and pH measurement:

- Provide best monitoring
- Easy calibration
- Self-cleaning
- Due to its extremely small size, it offers improved efficiency with respect to sample volume, reagent consumption and response time

Cons of continuous and invasive methods of blood gases and pH measurement:

- Potentially hazardous to patient
- There are stringent requirements for the sensor blood compatibility
- In vitro calibration is difficult
- Extreme miniaturization is required
- There is a packaging problem

This assignment has motivated us all to delve deeper into the field of blood gas sensing and even related fields. As the fusion of electronics and human body has seen a rise in interest over the last century, we are pretty sure that we've got lots of option to discover and study about.

6. Contributions:

Pranamya Jain (2018A8PS0769P): Severinghaus Sensor

Nitin Pant (2018A8PS0381P): Clark's Sensor

Ayush Agrawal (2018A8PS0769P): Combined Blood Gas Sensor

All members of the group had equal contribution (33.33%) in completion of this assignment.

7. References:

i. Severinghaus, J. W., & Bradley, A. F. (1958). Electrodes for blood pO2 and pCO2 determination. *Journal of applied physiology*, *13*(3), 515-520.

ii. Sørensen, P. R. (2005). Understanding the principles behind blood gas sensor technology.

iii. Arquint, P., Van den Berg, A., Van der Schoot, B. H., De Rooij, N. F., Bühler, H., Morf, W. E., & Dürselen, L. F. J. (1993). Integrated blood-gas sensor for pO2, pCO2 and pH. *Sensors and Actuators B: Chemical*, *13*(1-3), 340-344.

iv. Arquint, P., Van der Schoot, B. H., & de Rooij, N. F. (1995). Combined Blood Gas Sensor for pO 2, pCO 2 and pH. In *Micro Total Analysis Systems* (pp. 191-194). Springer, Dordrecht.

v. Zosel, J., Oelßner, W., Decker, M., Gerlach, G., & Guth, U. (2011). The measurement of dissolved and gaseous carbon dioxide concentration. *Measurement Science and Technology*, *22*(7), 072001.

vi. Manole, A., Neacsu, I., Apostu, M. O., & Melnig, V. (2006). Membrane covered polarographic oxygen sensor manufacturing. Theoretical considerations. *Analele Stiint Ale Univ*, *11*, 25-34.

vii. Breathnach, C. S. (1972). The development of blood gas analysis. *Medical history*, *16*(1), 51-62.

viii. Principles of measuring PCO_2 with the Severinghaus electrode | Deranged Physiology. (2015, August 6). Deranged Physiology. https://derangedphysiology.com/main/cicm-primary-exam/required-reading/respiratory-system/Chapter%20423/principles-measuring-pco2-severinghaus-electrode

ix. Meyerhoff, M. E. (1993). In vivo blood-gas and electrolyte sensors: Progress and challenges. *TrAC Trends in Analytical Chemistry*, *12*(6), 257-266.

x. Chang, S. C., Stetter, J. R., & Cha, C. S. (1993). Amperometric gas sensors. *Talanta*, *40*(4), 461-477.